Trapped Energetic Electrons in the Magnetosphere of Ganymede

Aharon Eviatar
Department of Geophysics and Planetary Sciences, The Raymond and Beverly Sackler Faculty of Exact Sciences, Tel Aviv University, Ramat Aviv, Israel

Donald J. Williams, Chris Paranicas, Richard W. McEntire and Barry H. Mauk
Applied Physics Laboratory, The Johns Hopkins University, Laurel, MD

Margaret G. Kivelson
Institute of Geophysics and Department of Earth and Space Sciences, University of California,Los Angeles

Abstract. On May 7, 1997, the Galileo orbiter flew through the magnetosphere of Ganymede and crossed flux tubes connected at both ends to the satellite. Energetic electrons, observed during this encounter by means of the Energetic Particle Detector on board Galileo, showed double loss cones and "butterfly" type pitch angle distributions, as has been noted in past publications. In addition, as the spacecraft flew toward Ganymede, both the shape and magnitude of the spectrum changed. The intensities decreased, with the greatest depletion observed at the lowest energies, and the monotonic slope characteristic of the Jovian environment was replaced by a rollover of the spectrum at the low-energy end. The spectra lead us to infer a strongly energy-dependent injection efficiency into the trapping region. As on previous encounters, the pitch angle distributions confirmed the position of the magnetopause as indicated by the magnetometer measurements, but the spectra remained Jovian until the trapping region was reached. Various physical mechanisms capable of generating the observed spectra and pitch angle distributions, including downstream reconnection insertion followed by magnetic gradient drift and absorption of the lowest-energy electrons by Ganymede and injection from Jovian flux tubes upstream are assessed.

1. Introduction

On May 5, 1997, the Galileo spacecraft, on its eighth orbit around Jupiter, encountered the satellite Ganymede (encounter G8). During this encounter the spacecraft entered a region of closed field lines as indicated by the detection of trapped energetic electrons [*Williams et al.*, 1997]. The model derived from the magnetometer measurements by *Kivelson et al.* [1998] is also consistent with the crossing of closed field lines by Galileo.

The above mentioned energetic electrons exhibit interesting pitch angle and spatial distributions [*Williams et al.*, 1997] and unusual spectral characteristics, which will be shown below. Their double loss cones and "butterfly" type pitch angle distributions are what indicate the closed nature of the field lines. As the spacecraft flew inward, toward Ganymede, both the shape and

Paper number 1999JA900450.
0149-0227/99/1999JA00$09.00

magnitude of the spectrum changed. The intensities decreased, with the greatest depletion observed at the lowest energies, and the monotonic slope characteristic of the Jovian environment was replaced by a rollover at a radial distance of $1.72\,R_g$. The depletion and spectral shape variation together with the size of the loss cones characterize particles with two mirror points in the magnetosphere of Ganymede. The former factors also lead us to infer a strongly energy dependent injection efficiency into the trapping region. In the following sections, we shall present the data and propose a physical mechanism that may be responsible for the observed phenomena

2. Ganymede Magnetic Field

The magnetic field of Earth's magnetosphere, originally described by *Dungey* [1961], is well approximated as a superposition of a dipole field and a uniform field strongly distorted in the direction of the flow of the solar wind. *Schulz* [1991], noting that the topology of the field is invariant if the flow effects are neglected, provided a useful expression for the scalar potential that represents the sum of a dipole field and a uniform field (aligned with the dipole moment) from which the vacuum magnetic field can be derived. This model has the feature that field lines inside a separatrix are closed and those outside of it are open. This is simply the standard procedure of superimposing a constant field, parallel to the dipole moment in the equatorial plane and attributed to magnetopause currents on the dipole field, which itself is taken to be aligned with the rotation axis [*Mead*, 1964]. Application of this model to Ganymede is, in effect, a simplification of a model published by *Kivelson et al.* [1998] in which the field is taken to be the sum of a tilted dipole and a uniform external field, tilted with respect to the dipole in a manner consistent with the Jovian field configuration at the time of the encounter. *Volwerk et al.* [1999] have used this more realistic field, with the addition of an image dipole to compensate for the flow distortion, to compute ion trajectories in the Ganymagnetosphere.

In a spherical coordinate system in which r is Ganycentric radial distance and θ is the magnetic colatitude,

$$V(r,\theta) = g_1^0 \cos\theta \left[\left(\frac{a^3}{r^2} \right) + 2 \left(\frac{a}{b} \right)^3 r \right] \tag{1}$$

where in our case, $a = 2634$ km is the radius of Ganymede, b is the magnetopause distance, and g_1^0 is the dipole coefficient in a spherical harmonic analysis of the potential. The field itself if given by

$$\vec{B}_G = -\nabla V.$$

We obtain thus the field components inside the Ganymede magnetosphere:

$$
\begin{aligned}
B_{Gr} &= 2g_1^0 \cos\theta \left(\frac{a}{r}\right)^3 \left[1 - \left(\frac{r}{b}\right)^3\right] \\
B_{G\theta} &= g_1^0 \sin\theta \left(\frac{a}{r}\right)^3 \left[1 + 2\left(\frac{r}{b}\right)^3\right].
\end{aligned} \tag{2}
$$

The equation of a field line for $r \leq b$ is

$$
\frac{2r}{a \sin^2\theta \left[2 + \left(\frac{r}{b}\right)^3\right]} = L, \tag{3}
$$

where L is the usual magnetic parameter and will reduce to the normal dipole L in the limit of $b- > \infty$. For $r > b$, outside the magnetosphere, we have

$$
\rho_\infty^2 = \frac{b^3}{r}\left[2 + \left(\frac{r}{b}\right)^3\right]\sin^2\theta \tag{4}
$$

in which ρ_∞ is the asymptotic distance between the field line and the "tail" axis of Ganymede.

The model shown in Figure 1 is a good approximation to the field configuration for the G8 encounter in which the local field of Jupiter's magnetosphere was almost aligned with the dipole moment of Ganymede. **Figure 1.**

3. Pitch Angle Distributions

The electron pitch angle distributions observed during the entry phase of the G8 encounter with Ganymede are of the type shown in Figure 2, which are flat, with a small loss cone on the Jupiter side and a larger one on the Ganymede side. For lower energies the Jupiter side loss cone is full, whereas for the higher energies it is empty as pointed out by *Williams and Mauk* [1997]. They evolve, as the spacecraft flies inward, to become of the butterfly type shown in Figure 3, with minima at 90° and large loss cones on both sides, as reported by *Williams et al.* [1997]. **Figure 2.** **Figure 3.**

The solid line in Figure 3 represents the model that we have chosen to fit the butterfly distribution:

$$
f(\alpha) = (\sin^2\alpha - M)(\cos^2\alpha + M), \tag{5}
$$

where $M = \sin^2\alpha_c$ is the mirror ratio. The total distribution is taken to be the gyrotropic function:

$$
F(p, \alpha) = f(\alpha) g(p), \tag{6}
$$

where $g(p)$ is an isotropic function bearing the energy spectrum. This is a simplification of a distribution introduced by *de Pater et al.* [1997] to model synchrotron emitting electrons near Amalthea.

Such distributions have long been known in the magnetosphere of the Earth [*Williams et al.*, 1973; *West et al.*, 1973] and have been shown to be a consequence of drift shell splitting [*Roederer*, 1968; *Pfitzer et al.*, 1969; *Sibeck et al.*, 1987]. A cartoon by *Williams et al.* [1997]

that illustrates how such distributions could evolve in the magnetosphere of Ganymede is shown in Figure 4. *Schulz* [1972] has calculated the rate of such splitting, *i.e.* the ratio of pitch angle scattering to the rate of radial diffusion for arbitrary pitch angle. **Figure 4.**

4. Energetic Electron Spectra

The electron spectra can be seen to vary significantly as the spacecraft moves across the Ganymede magnetosphere onto closed field lines, as may be noted in the time-color-coded Plates 1 and 2. We note that not only did the magnitude of the intensity decrease as the spacecraft entered the region of trapped particles, but the shape of the spectrum changed sharply as well. An across-the-board decrease could have been expected since the capacity of the small magnetosphere of Ganymede for trapping radiation belt particles is expected to be less than that of Jupiter, i.e., the *Kennel and Petschek* [1966] limit will be lower, but the energy dependence raises a more complex and interesting issue. The lowest-energy channel showed a depletion of ~ 3 orders of magnitude while the highest channel had a much smaller depletion, of about a factor of 4. In Figure 5 we see that the relative depletion is more or less linear in energy, which suggests magnetic gradient drift, the speed of which varies linearly with energy, as the factor determining the residence lifetimes of Ganymede magnetosphere energetic electrons. **Plate 1.** **Plate 2.** **Figure 5.**

In the absence of lower energy electron data for this epoch it is not possible to determine whether the rollover in the spectrum indicates a very low density of thermal plasma in this region as inferred by *Volwerk et al.* [1999]. We shall discuss in the next section possible mechanisms for generating the observed energetic electron spectra.

5. Electron Drift Paths

The motion of electrons injected at the downstream reconnection point will consist of a drift caused by the magnetic field gradient, which is energy dependent, and convection of the cross-magnetosphere electric field induced by the external corotation flow, which is not. This electric field will map into the magnetosphere of Ganymede with an efficiency ϵ taken to be of order 0.5 on the basis of the argument of *Kivelson et al.* [1998] that reconnection at Ganymede is very efficient.

We consider two extreme cases of the electric field transport mechanism, while realizing that reality will reside somewhere between them. In the first one we take Ganymede and/or its ionosphere to be an ideal conductor which requires that the potential associated with the electric field vanish on the surface of Ganymede. If the ionosphere is not exospheric, then the potential will vanish on the putative top of the ionosphere, one scale height above the surface. While this is not an obviously good approximation, the conductance of the Ganymede body and atmosphere-ionosphere system has been inferred by *Eviatar et al.* [1998] to be at least as high as $\approx 10^{-7}$mho, on the basis of deceleration of the corotation flow. This inference is, however, valid only for the polar regions of Ganymede which are magnetically connected to Jupiter [*Johnson*, 1997; *Williams et al.*, 1998]. If, however, Ganymede indeed exercises a degree of control over the low-frequency decametric emissions of Jupiter [*Menietti et al.*, 1998], in analogy to the control exercised by Io, then there must be sufficient conductance in the moon and atmosphere as a whole to close the needed current systems. At lower latitudes, the atmosphere should be less ionized [*Pappalardo et al.*, 1997], although ultraviolet spectroscopy of the surface [*Hendrix et al.*, 1999] indicates that charged particle-produced ozone may have a broader than expected latitude distribution. For our second model we assume a nonconducting Ganymede, which may correspond better to the equatorial regions which map to closed field lines.

The electric field potential imposed for the high conductance case will be that used by *Schulz and Eviatar* [1977], which vanishes at the surface of Ganymede, whereas for the insulating case the electric potential function is taken to be that used by *Schulz* [1991] and by *Volland* [1984], who dealt with the terrestrial magnetotail field, namely that imposed by a uniform external field on a dielectric cylinder. These investigators found that a quadratic potential is the most appropriate power of L. We may express the electric potential energy inside the closed field line region thus

$$\begin{array}{lllll} \psi & = & \sqrt{3}qE_J b \left(\frac{r-a}{r_x}\right)^2 \sin\phi & \sigma = \infty \\ \psi & = & \sqrt{3}qE_J b \left(\frac{r}{r_x}\right)^2 \sin\phi & \sigma = 0 \end{array} \tag{7}$$

in which, E_J is the Jovian corotation electric field taken to be $18\,\mathrm{m}V/m$ [*Volwerk et al.*, 1999] and $r_x \approx 1.8\,\mathrm{a}$ is the equatorial distance of the outermost closed field line. For $r > r_x/a$ the electric potential goes over continuously to [*Schulz*, 1991]

$$\psi = \sqrt{3}qE_J b \left(\frac{r_x}{r}\right)^{\frac{1}{2}} \sin\phi.$$

For particles moving thus, under the influence of a convection electric field and magnetic field gradient drift, with conservation of the magnetic moment μ and vanishing second invariant, the path of motion will be along the equipotentials of the Hamiltonian [*Schulz and Eviatar*, 1977]:

$$\begin{aligned} H &= \left(1 + \frac{\mu B}{m_0 c^2}\right)^{\frac{1}{2}} - 1 + \frac{\psi}{m_0 c^2} \\ &= \left(1 + \frac{\mu B_G}{m_0 c^2}\right)^{\frac{1}{2}} - 1 + \frac{\psi_G}{m_0 c^2} \end{aligned} \tag{8}$$

in which m_0c^2 is the electron rest energy and B_G and ψ_G are the magnetic field and electric potential energy at the surface of Ganymede. In Figures 6 and 7, which show the trajectories for various values of magnetic moment and conductivity, we can see the dependence on energy of the accessibility of the region traversed by the spacecraft during the close encounter. The conserved magnetic moment values used to characterized the various panels of Figures 6 and 7 are taken from combining the geometric mean of the energy in the various Energetic Particle Detector (EPD) channels with the observed magnetic field magnitude of ~ 150 nT at the point of observation [*Kivelson et al.*, 1998]. In (8), the magnetic moment is conserved and the magnetic field is the gradient of the scalar potential given by (1). The contours were chosen for clarity.

Figure 6.
Figure 7.

We can see that for the lowest-energy particles being convected upstream towards the moon, there will be an umbra behind Ganymede as noted by *Volwerk et al.* [1999]. For an electric potential vanishing on Ganymede, thermal electrons indeed will not reach the moon except for the singular $y = 0$ orbit, but neither will they achieve closed orbits and they will drift to the magnetopause and out to the Jupiter plasma sheet. The inability of the thermal ($\mu = 0$) particles to reach the upstream region is consistent with the inference of *Volwerk et al.* [1999] that the total plasma density there will be very low [*Kivelson et al.*, 1998]. The energy of these particles is in the range of the thermal plasma instrument and we may anticipate with some degree of confidence that the plasma and wave data in this region, when published, will indeed show a low density.

In order to make the graphs more legible, we have plotted only the the cold plasma, the lowest EPD channel, an intermediate energy and the highest energy. The conclusions do not differ from what is inferred from viewing all eight energy ranges. For higher energy particles, for which the effect of the electric field and the conductivity of Ganymede are less relevant, there is eventually access to closed orbits around Ganymede and we can expect the depletion relative to the fluxes observed in the Jovian magnetosphere to be much weaker for these particles, as we can see in Plates 1 and 2 We note that closed orbits are attained in both conductivity model pictures, although the closed orbit appears at a lower energy for the high conductivity case. It is not obvious that we can draw any firm conclusions about the appropriateness of either conductivity assumption from these convection orbits. The above trajectories were calculated for particles moving in the magnetoequatorial plane of Ganymede.

6. Discussion

We have presented data that indicate clearly that the depletion of energetic electrons in the magnetosphere of Ganymede compared to the ambient Jovian environment is highly energy dependent. We also note that the decrease in electron fluxes is well correlated to the development of butterfly pitch angle distributions and that magnetic field gradient drift which affects mainly higher-energy particles can carry them to where they can gain access to closed drift trajectories. The lowest-energy particles, on the other hand, will be influenced by electric field drift and will be either carried into Ganymede or more effectively, convected out to the magnetopause and thus back to the magnetosphere of Jupiter. The choice of assumption for the electrical conductivity of Ganymede appears to be unconstrained by these results. It is doubtful indeed whether it is possible to assign a single conductivity to Ganymede and its atmosphere since the characteristics of the moon vary greatly over its surface [*Johnson*, 1997; *Hendrix et al.*, 1999].

The formation of butterfly distributions is a natural result of drift shell splitting [*Pfitzer et al.*, 1969; *Schulz*, 1972; *Sibeck et al.*, 1987] which together with pitch angle scattering can drive radial diffusion [*Roederer and Schulz*, 1969]. Thus the downstream injection mechanism with drift toward Ganymede [*Williams et al.*, 1997; *Volwerk et al.*, 1999] appears able to provide an explanation for the observed spectra and pitch angle distributions.

Acknowledgments. Helpful discussions with V.M. Vasyliūnas are gratefully acknowledged. The work at the University of California, Los Angeles was supported by the National Aeronautics and Space Administration through the Jet Propulsion Laboratory under contract JPL 958694. At the Johns Hopkins University Applied Physics Laboratory this research was supported by the National Aeronautics and Space Administration Galileo Program by means of contract N00039-95-0002 between the United States Department of the Navy and Johns Hopkins University. Work at Tel Aviv University was supported in part by the German-Israeli Foundation for Scientific Research and Development under grant I-562-242.07/97. A. Eviatar gratefully acknowledges the hospitality of the Johns Hopkins University Applied Physics Laboratory and of the Institute of Geophysics and Planetary Physics of the University of California, Los Angeles during the summer of 1998.

Janet G. Luhmann thanks John Doug Menietti and another referee for their assistance in evaluating this paper.

Figure 1. Schematic distorted magnetic field model analogous to terrestrial models [*Dungey*, 1961; *Schulz*, 1991] given by equation (3); The thick arrow at the center of Ganymede is the magnetic moment of the moon and the thin arrows are tangents to the local magnetic field lines, placed to emphasize the reconnection regions. View is from upstream in a plane normal to the Jovian equatorial plane and to the corotation flow. The projection of the Galileo trajectory on this plane is shown by the line of asterisks. The entrance and exit times are marked by arrows and diamond symbols.

Figure 2. Pitch angle distribution of electrons on the approach to Ganymede.

Figure 3. Pitch angle distribution of electrons near Ganymede for low and high Energetic Particle Detector energy channels. The solid line is the "butterfly" function given in equation (5).

Figure 4. Cartoon of possible trajectories leading to shell splitting [*Williams et al.*, 1997]. (a) View from "above" of the equatorial trajectories on constant B surfaces and (b) a meridional view of the same configuration. Both Figures 4a and 4b are schematic.

Plate 1. Energetic Particle Detector electron spectra on the inbound leg: Ganymede 8.

Plate 2. Energetic Particle Detector electron spectra on the outbound leg: Ganymede 8.

Figure 5. Ratio of the electron intensities observed on Ganymede 8 at closest approach to those observed in the ambient Jovian magnetosphere just before crossing the Ganymede magnetopause, as a function of energy. The nearly 45° slope of the curves appears to implicate magnetic gradient drift in causing the observed phenomena.

Figure 6. Electron trajectories near Ganymede: infinite conductivity. The energy is represented by the conserved magnetic moment, the value of which is given in each graph.

Figure 7. Electron trajectories near Ganymede: zero conductivity. The energy is represented by the conserved magnetic moment, the value of which is given in each graph.

References

de Pater, I., M. Schulz, and S. H. Brecht, Synchrotron evidence for Amalthea's influence on Jupiter's radiation belt, *J. Geophys. Res.*, *102*, 22,043–22,064, 1997.

Dungey, J. W., Interplanetary magnetic field and the auroral zones, *Phys. Rev. Lett.*, *6*, 47–48, 1961.

Eviatar, A., A. F. Cheng, C. Paranicas, B. H. Mauk, R. W. McEntire, and D. J. Williams, Plasma flow in the magnetosphere of Ganymede, *Geophys. Res. Lett.*, *25*, 1257–1260, 1998.

Hendrix, A. R., C. A. Barth, and C. W. Hord, Ganymede's ozone-like absorber: Observations by the Galileo ultraviolet spectrometer, *J. Geophys. Res.*, *104*, 14,169–14,177, 1999.

Johnson, R. E., Polar "caps" on Ganymede and Io revisited, *Icarus*, *128*, 469–471, 1997.

Kennel, C. F., and H. E. Petschek, Limit on stably trapped particle fluxes, *J. Geophys. Res.*, *71*, 1–28, 1966.

Kivelson, M. G., J. Warnecke, L. Bennett, S. Joy, K. K. Khurana, J. A. Linker, C. T. Russell, R. J. Walker, and C. Polanskey, Ganymede's magnetosphere: Magnetometer overview, *J. Geophys. Res.*, *103*, 19,963–19,972, 1998.

Mead, G. D., Deformation of the geomagnetic field by the solar wind, *J. Geophys. Res.*, *69*, 1169–1179, 1964.

Menietti, J. D., D. A. Gurnett, W. S. Kurth, and J. B. Groene, Control of Jovian radio emission by Ganymede, *Geophys. Res. Lett.*, *25*, 4281–4284, 1998.

Pappalardo, R. T., et al., Ganymede tectonics: Insights from Galileo imaging, *Bull. Am. Astron. Soc.*, *29*, 989, 1997.

Pfitzer, K. A., T. W. Lezniak, and J. R. Winkler, Experimental verification of drift-shell splitting in the distorted magnetosphere, *J. Geophys. Res.*, *74*, 4687–4693, 1969.

Roederer, J. G., Shell splitting and radial diffusion of geomagnetically trapped particles, in *Earth's Particles and Fields*, edited by B. M. McCormac, pp. 193–198,, Reinhold, New York, 1968.

Roederer, J. G., and M. Schulz, Effect of shell splitting on radial diffusion in the magnetosphere, *J. Geophys. Res.*, *74*, 4117–4122, 1969.

Schulz, M., Drift-shell splitting at arbitrary pitch angle, *J. Geophys. Res.*, *77*, 624–634, 1972.

Schulz, M., The magnetosphere, in *Geomagnetism*, edited by J. A. Jacobs, vol. 4, chap. 2, pp. 87–293, Academic Press, San Diego, CA, 1991.

Schulz, M., and A. Eviatar, Charged particle absorption by Io, *Astrophys. J.*, *211*, L149–L154, 1977.

Sibeck, D. G., R. W. McEntire, A. T. Y. Lui, R. E. Lopez, and S. M. Krimigis, Magnetic field drift shell splitting: Cause of unusual dayside particle pitch angle distributions during storms and substorms, *J. Geophys. Res.*, *92*, 13,485–13,497, 1987.

Volland, H., *Atmospheric Electrodynamics*, Springer, New York, 1984.

Volwerk, M., M. G. Kivelson, K. K. Khurana, and R. L. McPherron, Probing Ganymede's magnetosphere with field line resonances, *J. Geophys. Res.*, *104*, 14,729–14,738, 1999.

West, H. I., R. M. Buck, and J. R. Walton, Electron pitch angle distributions throughout the magnetosphere as observed by Ogo 5, *J. Geophys. Res.*, *78*, 1064–1081, 1973.

Williams, D. J., and B. H. Mauk, Pitch angle diffusion at Jupiter's moon Ganymede, *J. Geophys. Res.*, *102*, 24,283–24,287, 1997.

Williams, D. J., T. A. Fritz, and A. Konradi, Observations of proton spectra ($1.0 \leq E_p \leq 300$ keV), *J. Geophys. Res.*, *78*, 4751–4755, 1973.

Williams, D. J., B. H. Mauk, and R. W. McEntire, Trapped electrons in Ganymede's magnetic field, *Geophys. Res. Lett.*, *24*, 2953–2956, 1997.

Williams, D. J., B. H. Mauk, and R. W. McEntire, Properties of Ganymede's magnetosphere as revealed by energetic particle observations, *J. Geophys. Res.*, *103*, 17,523–17,534, 1998.

(Received June 2, 1999; revised September 7,1999; accepted October 5, 1999.)

EVIATAR ET AL.:: GANYMEDE ENERGETIC ELECTRONS

EVIATAR ET AL.:: GANYMEDE ENERGETIC ELECTRONS

EVIATAR ET AL.:: GANYMEDE ENERGETIC ELECTRONS

EVIATAR ET AL.:: GANYMEDE ENERGETIC ELECTRONS

EVIATAR ET AL.:: GANYMEDE ENERGETIC ELECTRONS

EVIATAR ET AL.:: GANYMEDE ENERGETIC ELECTRONS

EVIATAR ET AL.:: GANYMEDE ENERGETIC ELECTRONS

EVIATAR ET AL.:: GANYMEDE ENERGETIC ELECTRONS

EVIATAR ET AL.:: GANYMEDE ENERGETIC ELECTRONS

A. Eviatar,Department of Geophysics and Planetary Sciences, The Raymond and Beverly Sackler Faculty of Exact Sciences, Tel Aviv University, POB 39040, Ramat Aviv, 69978 Tel Aviv, Israel(arkee@daphne.tau.ac.il)

B.H. Mauk, R.W. McEntire, C. Paranicas and D.J. Williams, Applied Physics Laboratory, The Johns Hopkins University, Laurel, MD 20742(barry.mauk@jhuapl.edu; richard.mcentire@jhuapl.edu; chris.paranicas@jhuapl.edu; donald.williams@jhuapl.edu)

M.G. Kivelson, Institute of Geophysics and Department of Earth and Space Sciences, University of California,Los Angeles, CA 90024(mkivelson@igpp.ucla.edu)

Figure Captions

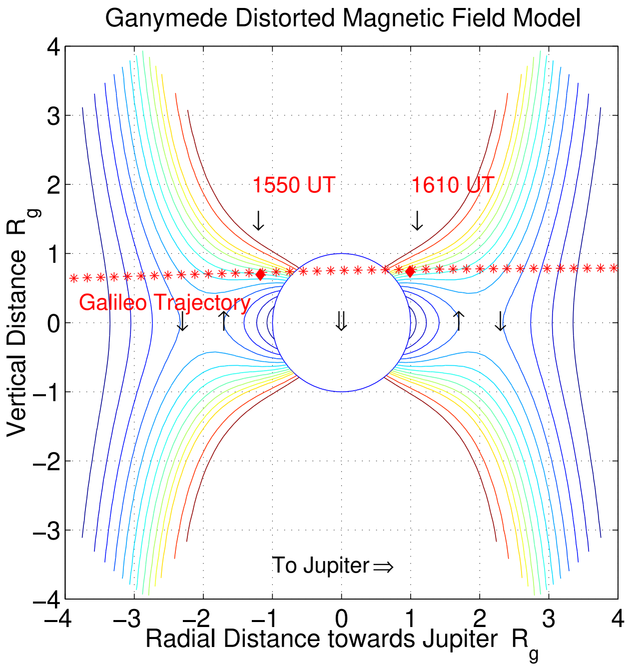

Figure 1. Schematic distorted magnetic field model analogous to terrestrial models [*Dungey*, 1961; *Schulz*, 1991] given by equation (3); The thick arrow at the center of Ganymede is the magnetic moment of the moon and the thin arrows are tangents to the local magnetic field lines, placed to emphasize the reconnection regions. View is from upstream in a plane normal to the Jovian equatorial plane and to the corotation flow. The projection of the Galileo trajectory on this plane is shown by the line of asterisks. The entrance and exit times are marked by arrows and diamond symbols.

Figure 1. Schematic distorted magnetic field model analogous to terrestrial models [*Dungey*, 1961; *Schulz*, 1991] given by equation (3); The thick arrow at the center of Ganymede is the magnetic moment of the moon and the thin arrows are tangents to the local magnetic field lines, placed to emphasize the reconnection regions. View is from upstream in a plane normal to the Jovian equatorial plane and to the corotation flow. The projection of the Galileo trajectory on this plane is shown by the line of asterisks. The entrance and exit times are marked by arrows and diamond symbols.

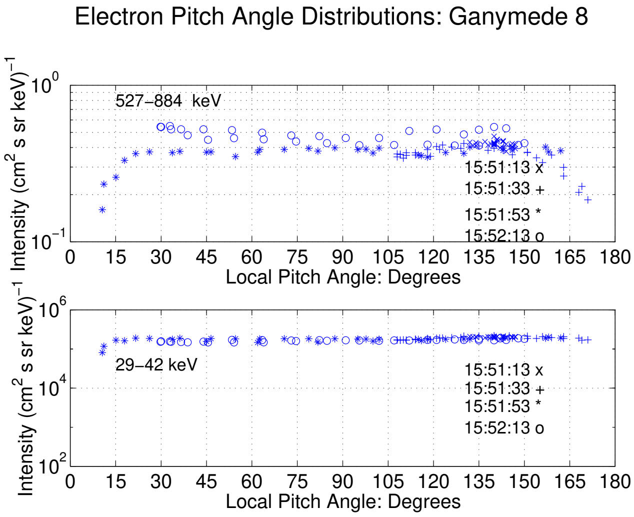

Figure 2. Pitch angle distribution of electrons on the approach to Ganymede.

Figure 2. Pitch angle distribution of electrons on the approach to Ganymede.

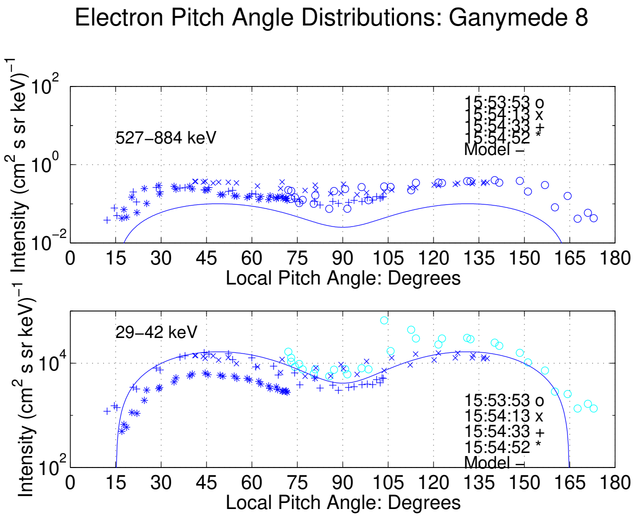

Figure 3. Pitch angle distribution of electrons near Ganymede for low and high Energetic Particle Detector energy channels. The solid line is the “butterfly” function given in equation 5

Figure 3. Pitch angle distribution of electrons near Ganymede for low and high Energetic Particle Detector energy channels. The solid line is the “butterfly” function given in equation 5

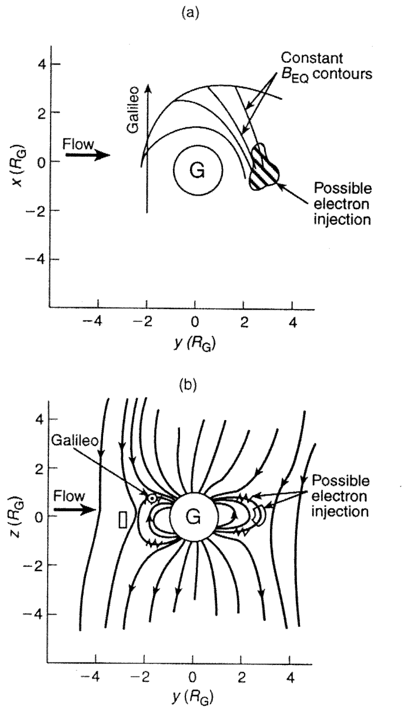

Figure 4. Cartoon of possible trajectories leading to shell splitting [*Williams et al.*, 1997]. (a) View from "above" of the equatorial trajectories on constant B surfaces and (b) a meridional view of the same configuration. Both Figures 4a 4b are schematic.

Figure 4. Cartoon of possible trajectories leading to shell splitting [*Williams et al.*, 1997]. (a) View from "above" of the equatorial trajectories on constant B surfaces and (b) a meridional view of the same configuration. Both Figures 4a 4b are schematic.

G8 EPD Electron Spectra and Distribution Functions

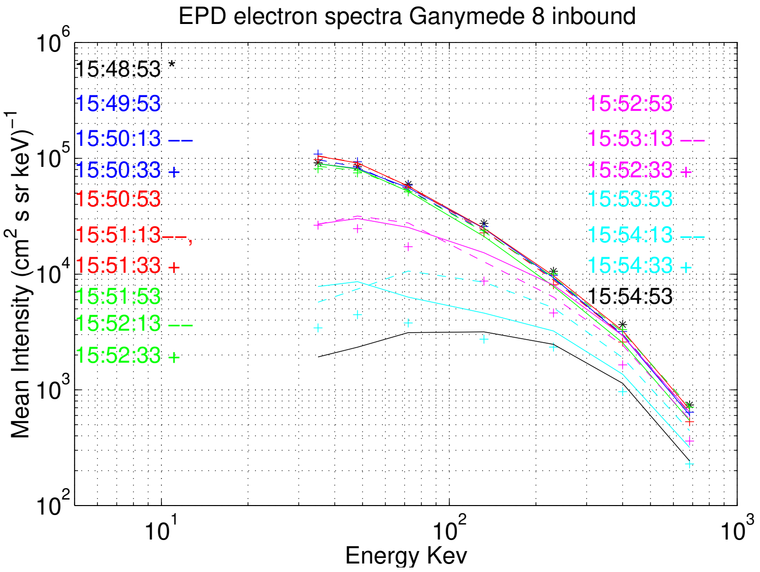

Plate 1. Energetic Particle Detector electron spectra on the inbound leg: Ganymede 8.

Plate 1. Energetic Particle Detector electron spectra on the inbound leg: Ganymede 8.

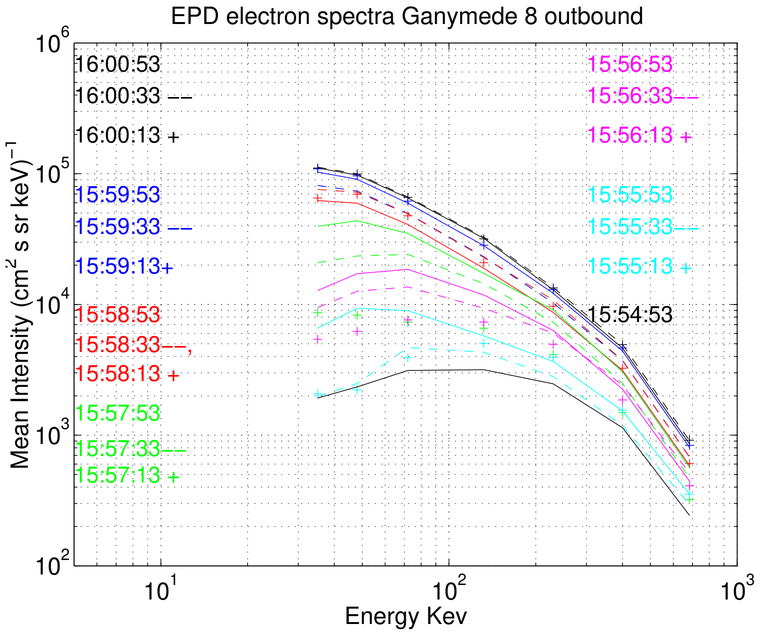

Plate 2. Energetic Particle Detector electron spectra on the outbound leg: Ganymede 8.

Plate 2. Energetic Particle Detector electron spectra on the outbound leg: Ganymede 8.

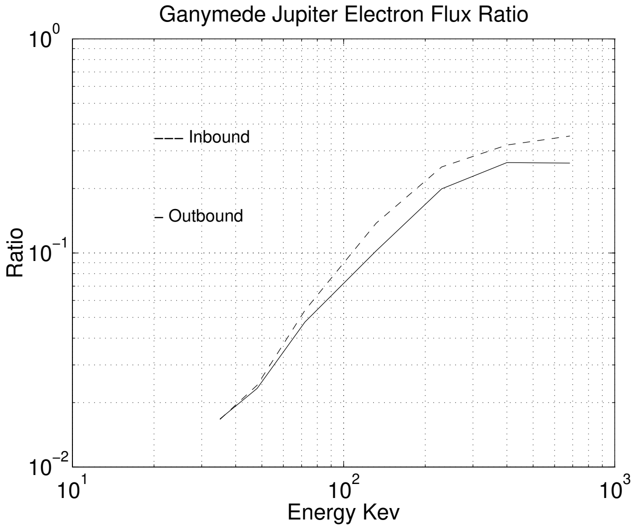

Figure 5. Ratio of the electron intensities observed on Ganymede 8 at closest approach to those observed in the ambient Jovian magnetosphere just before crossing the Ganymede magnetopause, as a function of energy. The nearly 45° slope of the curves appears to implicate magnetic gradient drift in causing the observed phenomena.

Figure 5. Ratio of the electron intensities observed on Ganymede 8 at closest approach to those observed in the ambient Jovian magnetosphere just before crossing the Ganymede magnetopause, as a function of energy. The nearly 45° slope of the curves appears to implicate magnetic gradient drift in causing the observed phenomena.

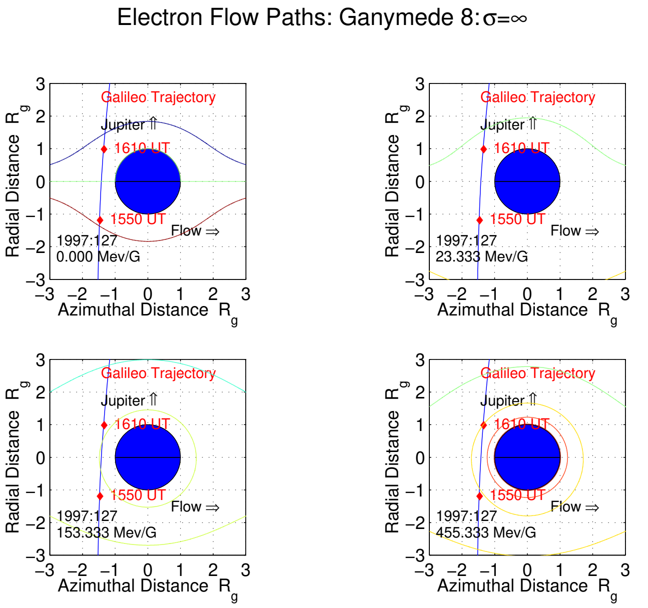

Figure 6. Electron trajectories near Ganymede: infinite conductivity. The energy is represented by the conserved magnetic moment, the value of which is given in each graph.

Figure 6. Electron trajectories near Ganymede: infinite conductivity. The energy is represented by the conserved magnetic moment, the value of which is given in each graph.

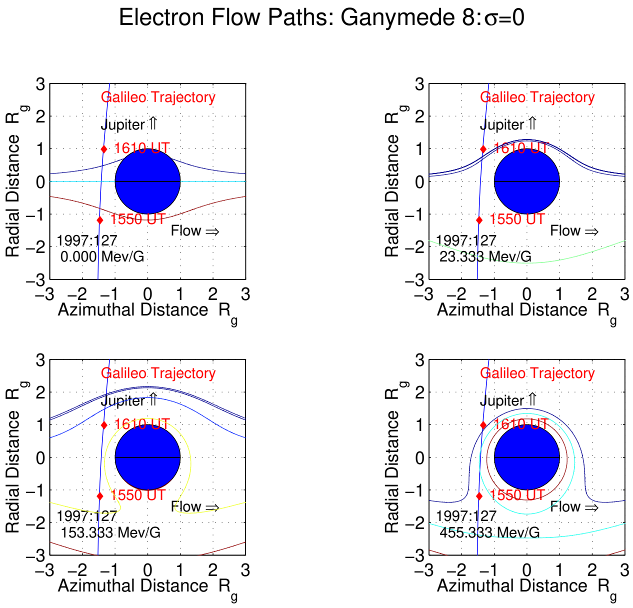

Figure 7. Electron trajectories near Ganymede: zero conductivity. The energy is represented by the conserved magnetic moment, the value of which is given in each graph.

Figure 7. Electron trajectories near Ganymede: zero conductivity. The energy is represented by the conserved magnetic moment, the value of which is given in each graph.

Figures

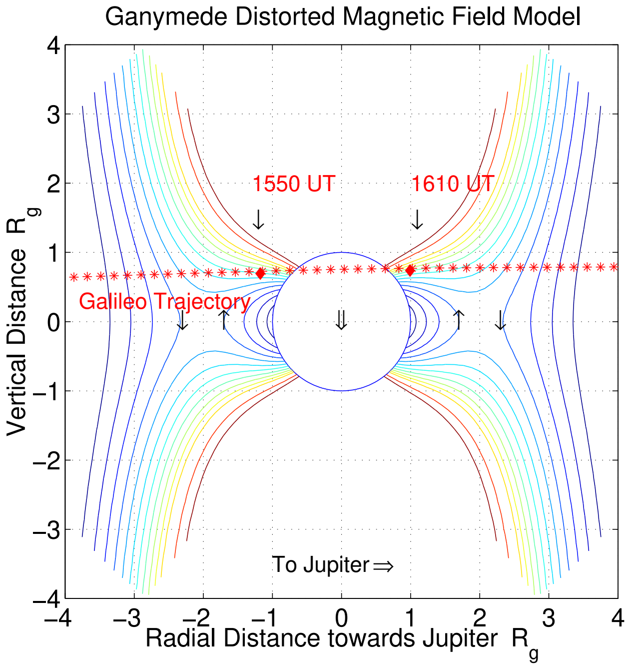

Figure 1. Schematic distorted magnetic field model analogous to terrestrial models [*Dungey*, 1961; *Schulz*, 1991] given by equation (3); The thick arrow at the center of Ganymede is the magnetic moment of the moon and the thin arrows are tangents to the local magnetic field lines, placed to emphasize the reconnection regions. View is from upstream in a plane normal to the Jovian equatorial plane and to the corotation flow. The projection of the Galileo trajectory on this plane is shown by the line of asterisks. The entrance and exit times are marked by arrows and diamond symbols.

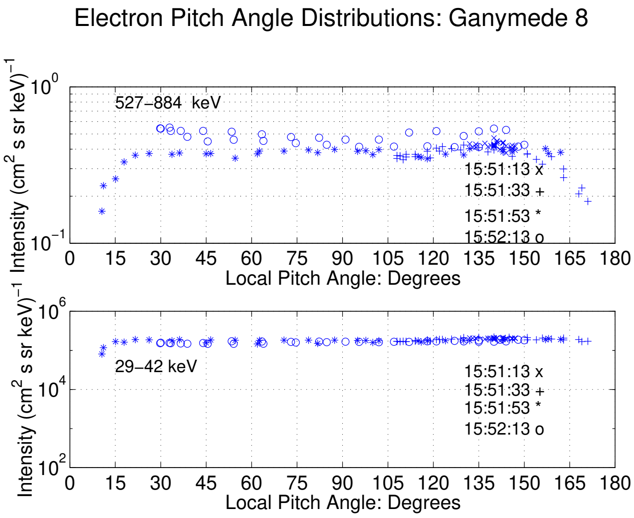

Figure 2. Pitch angle distribution of electrons on the approach to Ganymede.

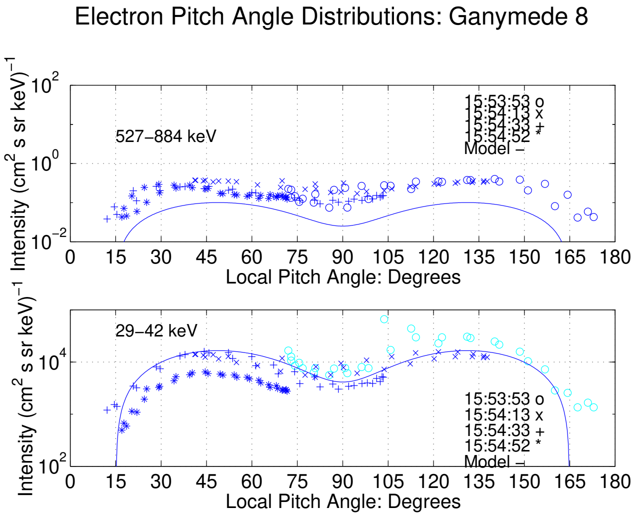

Figure 3. Pitch angle distribution of electrons near Ganymede for low and high Energetic Particle Detector energy channels. The solid line is the "butterfly" function given in equation 5

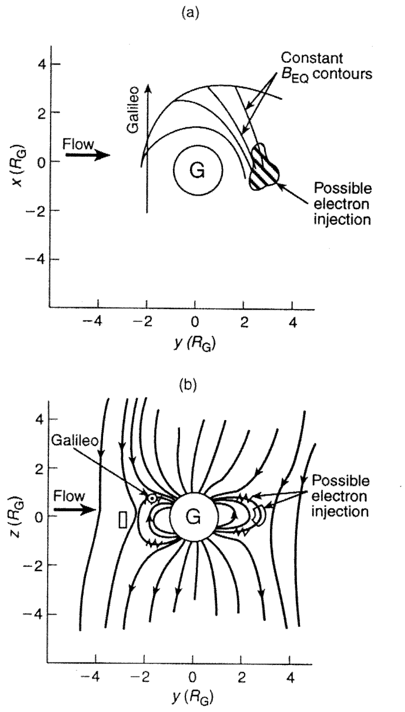

Figure 4. Cartoon of possible trajectories leading to shell splitting [*Williams et al.*, 1997]. (a) View from "above" of the equatorial trajectories on constant B surfaces and (b) a meridional view of the same configuration. Both Figures 4a 4b are schematic.

G8 EPD Electron Spectra and Distribution Functions

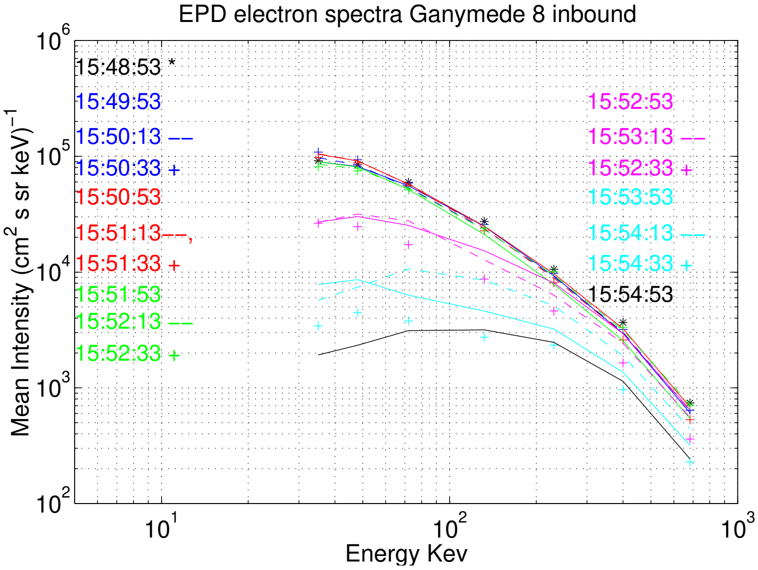

Plate 1. Energetic Particle Detector electron spectra on the inbound leg: Ganymede 8.

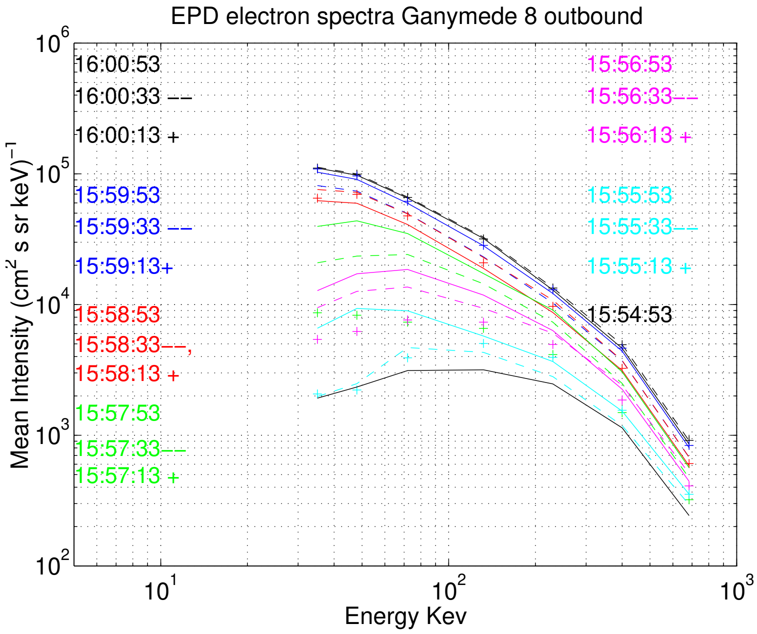

Plate 2. Energetic Particle Detector electron spectra on the outbound leg: Ganymede 8.

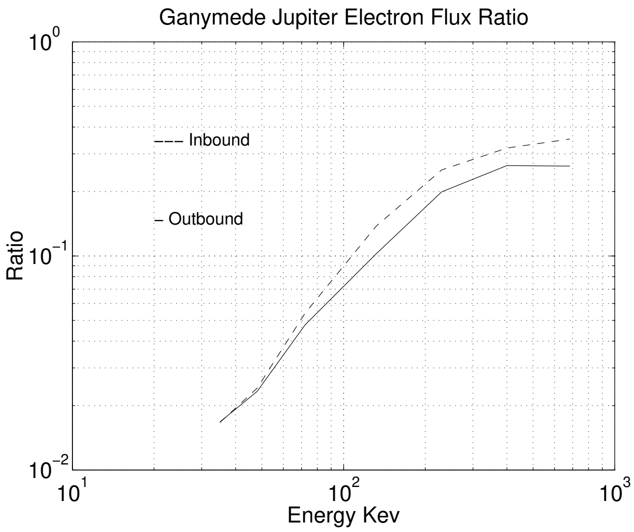

Figure 5. Ratio of the electron intensities observed on Ganymede 8 at closest approach to those observed in the ambient Jovian magnetosphere just before crossing the Ganymede magnetopause, as a function of energy. The nearly 45° slope of the curves appears to implicate magnetic gradient drift in causing the observed phenomena.

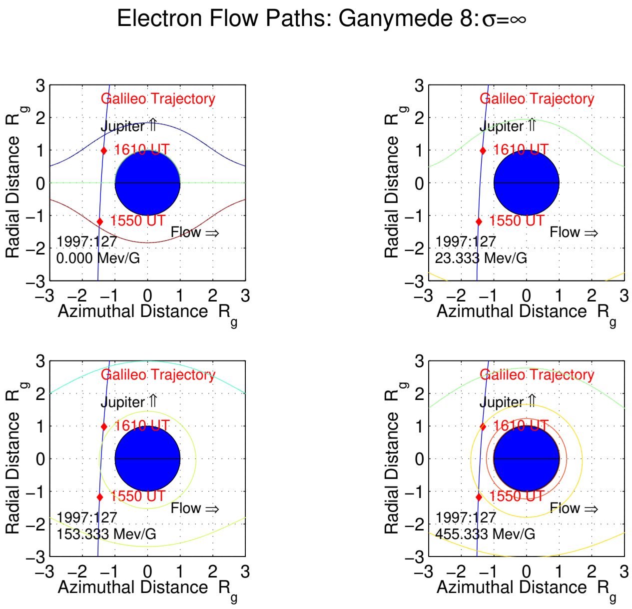

Figure 6. Electron trajectories near Ganymede: infinite conductivity. The energy is represented by the conserved magnetic moment, the value of which is given in each graph.

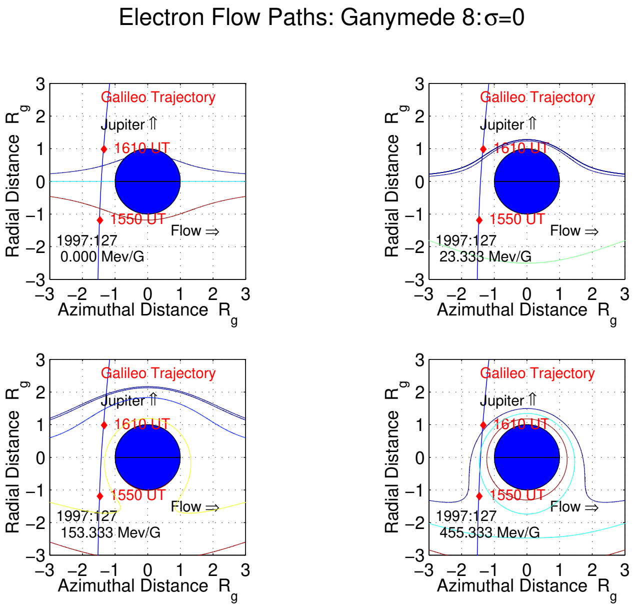

Figure 7. Electron trajectories near Ganymede: zero conductivity. The energy is represented by the conserved magnetic moment, the value of which is given in each graph.

Paper number 1999JA900450

On May 7, 1997, the Galileo orbiter flew through the magnetosphere of Ganymede and crossed flux tubes connected at both ends to the satellite. Energetic electrons, observed during this encounter by means of the Energetic Particle Detector on board Galileo, showed double loss cones and "butterfly" type pitch angle distributions, as has been noted in past publications. In addition, as the spacecraft flew toward Ganymede, both the shape and magnitude of the spectrum changed. The intensities decreased, with the greatest depletion observed at the lowest energies, and the monotonic slope characteristic of the Jovian environment was replaced by a rollover of the spectrum at the low-energy end. The spectra lead us to infer a strongly energy-dependent injection efficiency into the trapping region. As on previous encounters, the pitch angle distributions confirmed the position of the magnetopause as indicated by the magnetometer measurements, but the spectra remained Jovian until the trapping region was reached. Various physical mechanisms capable of generating the observed spectra and pitch angle distributions, including downstream reconnection insertion followed by magnetic gradient drift and absorption of the lowest-energy electrons by Ganymede and injection from Jovian flux tubes upstream are assessed.